

Electronic Supporting Information

**Assembly of Heterobimetallic $\text{Ni}^{\text{II}}\text{-Ln}^{\text{III}}$ ($\text{Ln}^{\text{III}} = \text{Dy}^{\text{III}}, \text{Tb}^{\text{III}}, \text{Gd}^{\text{III}}, \text{Ho}^{\text{III}}, \text{Er}^{\text{III}}, \text{Y}^{\text{III}}$) Complexes Using a Ferrocene Ligand:
Slow Relaxation of the Magnetization in Dy^{III} , Tb^{III} and Ho^{III}
Analogues**

AmitChakraborty,^aPrasenjitBag,^a Eric Rivière,^bTalalMallah^b, VadapalliChandrasekhar^{a,c}

^aDepartment of Chemistry, Indian Institute of Technology Kanpur, Kanpur-208016, India

^bInstitut de ChimieMoleculaire et Mate riaux d'Orsay, Universite Paris-Sud 11, F-91405, Orsay,
France

^cNational Institute of Science Education and Research, Institute of Physics Campus,
SachivalayaMarg, Sainik School Road, Bhubaneshwar-751 005, Odisha, India

Table S1.

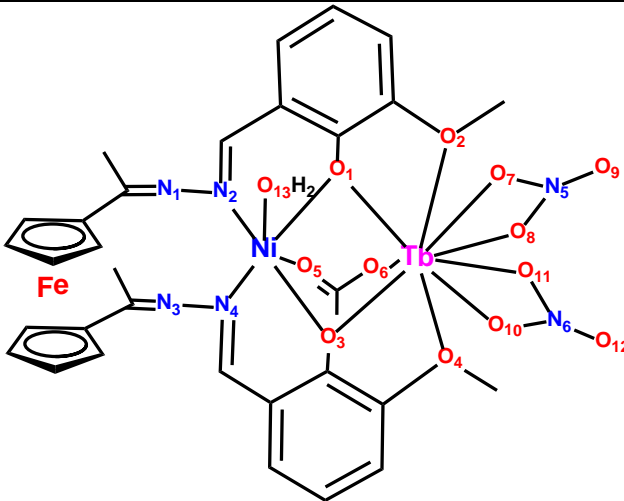
	Bond lengths around Terbium(III) (Å)	Bond angles around Terbium(III) (°)
Tb(1)-O(6) 2.304(5)	O(3)-Tb(1)-O(1) 70.05(18)	
Tb(1)-O(3) 2.320(5)	O(3)-Tb(1)-O(4) 63.70(18)	
Tb(1)-O(1) 2.331(5)	O(1)-Tb(1)-O(2) 62.49(17)	
Tb(1)-O(8) 2.423(6)	O(4)-Tb(1)-O(2) 140.02(19)	
Tb(1)-O(7) 2.460(7)		
Tb(1)-O(11) 2.467(6)		
Tb(1)-O(10) 2.499(6)		
Tb(1)-O(4) 2.529(6)		
Tb(1)-O(2) 2.613(6)		
Bond lengths around Nickel(II) (Å)	Bond angles around Nickel(II) (°)	
Ni(1)-O(5) 2.017(5)	O(3)-Ni(1)-O(1) 81.5(2)	
Ni(1)-O(3) 2.036(5)	O(1)-Ni(1)-N(2) 87.3(2)	
Ni(1)-O(1) 2.055(5)	O(3)-Ni(1)-N(4) 87.0(2)	
Ni(1)-N(2) 2.076(6)	N(2)-Ni(1)-N(4) 104.2(2)	
Ni(1)-O(13) 2.091(6)	Ni(1)-O(1)-Tb(1) 102.5(2)	
Ni(1)-N(4) 2.126(6)	Ni(1)-O(3)-Tb(1) 103.5(2)	

Table S2.

	Bond lengths around Holmium(III) (Å)	Bond angles around Holmium(III) (°)
	Ho(1)-O(6) 2.284(3) Ho(1)-O(3) 2.296(2) Ho(1)-O(1) 2.307(3) Ho(1)-O(8) 2.407(3) Ho(1)-O(10) 2.438(3) Ho(1)-O(7) 2.451(3) Ho(1)-O(11) 2.485(3) Ho(1)-O(4) 2.534(3) Ho(1)-O(2) 2.610(3)	O(3)-Ho(1)-O(1) 70.43(9) O(3)-Ho(1)-O(4) 63.97(9) O(1)-Ho(1)-O(2) 62.86(8) O(4)-Ho(1)-O(2) 139.00(9)
	Bond lengths around Nickel(II) (Å)	Bond angles around Nickel(II) (°)
	Ni(1)-O(5) 2.023(3) Ni(1)-O(3) 2.038(3) Ni(1)-O(1) 2.054(2) Ni(1)-N(2) 2.073(3) Ni(1)-O(13) 2.098(3)	O(3)-Ni(1)-O(1) 80.89(10) O(1)-Ni(1)-N(2) 87.84(11) O(3)-Ni(1)-N(4) 87.24(11) N(2)-Ni(1)-N(4) 103.94(11) Ni(1)-O(1)-Ho(1) 102.62(11) Ni(1)-O(3)-Ho(1) 103.49(11)

	Ni(1)-N(4) 2.130(3)	
--	---------------------	--

Table S3.

	Bond lengths around Gadolinium(III) (Å)	Bond angles around Gadolinium(III) (°)
	Bond lengths around Nickel(II) (Å)	Bond angles around Nickel(II) (°)
Gd(1)-O(6) 2.325(4)	O(1)-Gd(1)-O(3) 69.45(14)	
Gd(1)-O(1) 2.331(4)	O(1)-Gd(1)-O(2) 63.41(13)	
Gd(1)-O(3) 2.350(4)	O(3)-Gd(1)-O(4) 62.51(13)	
Gd(1)-O(8) 2.442(4)	O(2)-Gd(1)-O(4) 140.55(15)	
Gd(1)-O(7) 2.471(5)		
Gd(1)-O(11) 2.472(5)		
Gd(1)-O(10) 2.513(4)		
Gd(1)-O(2) 2.538(4)		
Gd(1)-O(4) 2.610(5)		
Bond lengths around Nickel(III) (Å)	O(1)-Ni(1)-O(3) 81.48(17)	
Ni(1)-O(5) 2.017(4)	O(3)-Ni(1)-N(4) 87.41(18)	
Ni(1)-O(1) 2.039(4)	O(1)-Ni(1)-N(2) 87.26(18)	
Ni(1)-O(3) 2.047(4)	N(4)-Ni(1)-N(2) 103.73(18)	
Ni(1)-N(4) 2.069(5)	Ni(1)-O(1)-Gd(1) 103.77(17)	
	Ni(1)-O(3)-Gd(1) 102.87(17)	

	Ni(1)-O(13) 2.094(4) Ni(1)-N(2) 2.127(5)	
--	---	--

Table S4.

	Bond lengths around Erbium(III) (Å)	Bond angles around Erbium(III) (°)
	Er(1)-O(6) 2.270(5) Er(1)-O(1) 2.278(6) Er(1)-O(3) 2.299(5) Er(1)-O(8) 2.385(6) Er(1)-O(7) 2.401(7) Er(1)-O(11) 2.425(6) Er(1)-O(10) 2.465(6) Er(1)-O(2) 2.520(6) Er(1)-O(4) 2.599(6)	O(1)-Er(1)-O(3) 70.6(2) O(1)-Er(1)-O(2) 64.27(19) O(3)-Er(1)-O(4) 62.80(19) O(2)-Er(1)-O(4) 138.79(19)
	Bond lengths around Nickel(II) (Å)	Bond angles around Nickel(II) (°)
	Ni(1)-O(5) 2.004(5) Ni(1)-O(1) 2.033(6) Ni(1)-O(3) 2.051(6) Ni(1)-O(13) 2.074(5) Ni(1)-N(4) 2.079(7) Ni(1)-N(2) 2.137(7)	O(1)-Ni(1)-O(3) 80.7(2) O(3)-Ni(1)-N(4) 87.7(2) O(1)-Ni(1)-N(2) 87.2(2) N(4)-Ni(1)-N(2) 104.4(3) Ni(1)-O(1)-Er(1) 103.8(3) Ni(1)-O(3)-Er(1) 102.5(3)

Table S5.

	Bond lengths around Yttrium (III) (Å)	Bond angles around Yttrium (III) (°)
	Y(1)-O(6) 2.277(2) Y(1)-O(1) 2.279(2) Y(1)-O(3) 2.299(2) Y(1)-O(8) 2.401(3) Y(1)-O(7) 2.434(3) Y(1)-O(10) 2.439(3) Y(1)-O(11) 2.473(2) Y(1)-O(2) 2.529(3) Y(1)-O(4) 2.596(3)	O(1)-Y(1)-O(2) 64.07(8) O(3)-Y(1)-O(4) 63.04(7) O(2)-Y(1)-O(4) 139.10(8) O(1)-Y(1)-O(3) 70.52(8)
Bond lengths around Nickel(II) (Å)	Bond angles around Nickel(II) (°)	
	Ni(1)-O(5) 2.020(2) Ni(1)-O(1) 2.036(2) Ni(1)-O(3) 2.043(2) Ni(1)-N(4) 2.069(3) Ni(1)-O(13) 2.086(2) Ni(1)-N(2) 2.123(3)	O(1)-Ni(1)-O(3) 80.77(9) O(1)-Ni(1)-N(2) 87.51(9) N(4)-Ni(1)-N(2) 103.76(10) O(3)-Ni(1)-N(4) 87.87(9) Ni(1)-O(1)-Y(1) 103.56(9) Ni(1)-O(3)-Y(1) 102.63(9)

	Y(1)-Ni(1) 3.3930(11)	
--	-----------------------	--

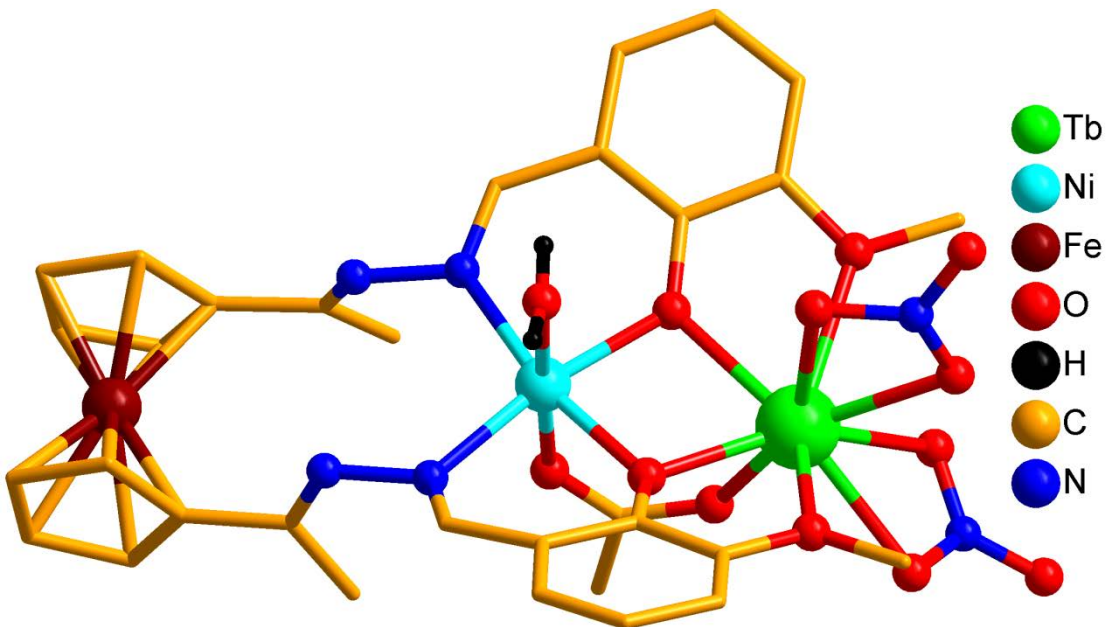


Figure S1. Molecular structure of **2**. Hydrogen atoms and solvent molecules are omitted for clarity.

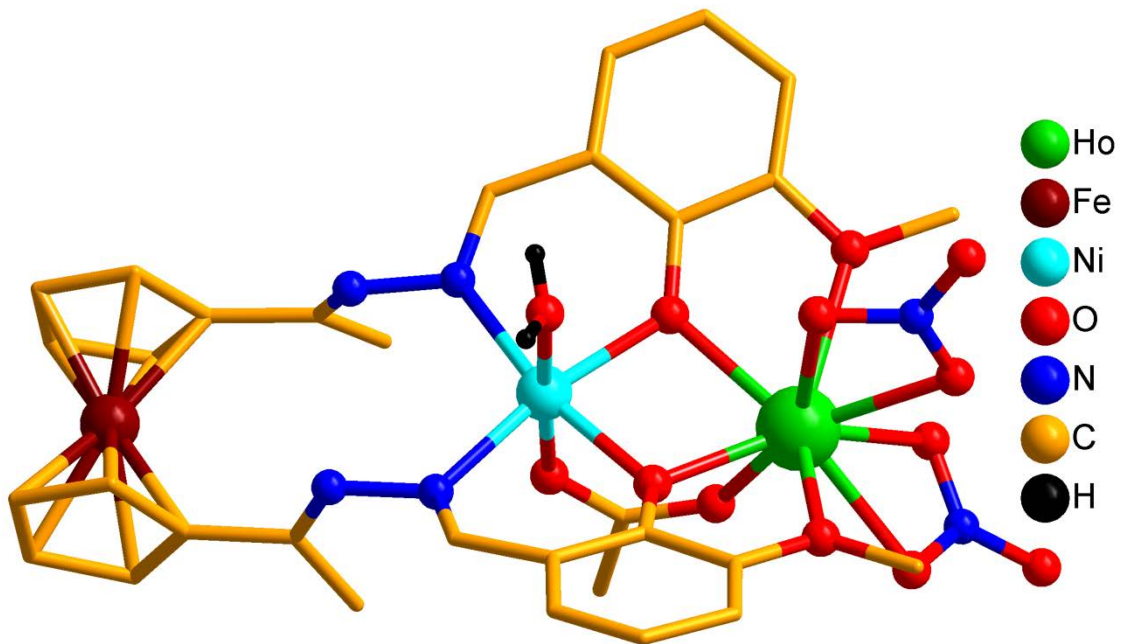


Figure S2. Molecular structure of **3**. Hydrogen atoms and solvent molecules are omitted for clarity.

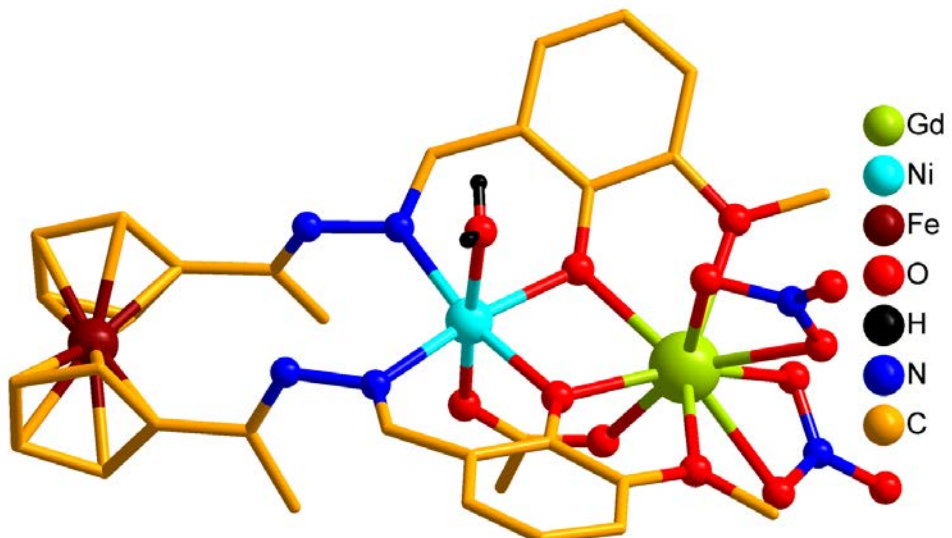


Figure S3. Molecular structure of **4**. Hydrogen atoms and solvent molecules are omitted for clarity.

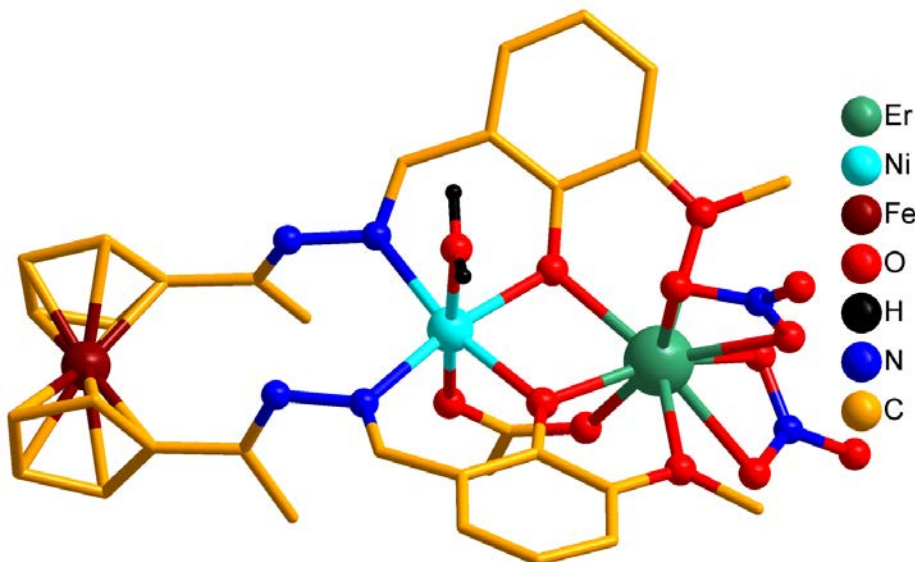


Figure S4. Molecular structure of **5**. Hydrogen atoms and solvent molecules are omitted for clarity.

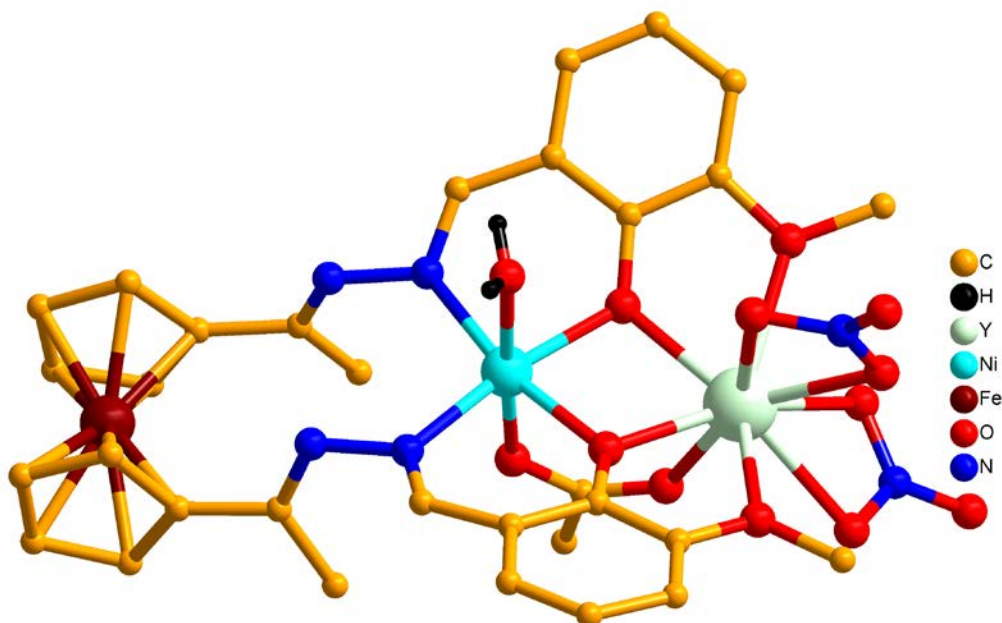
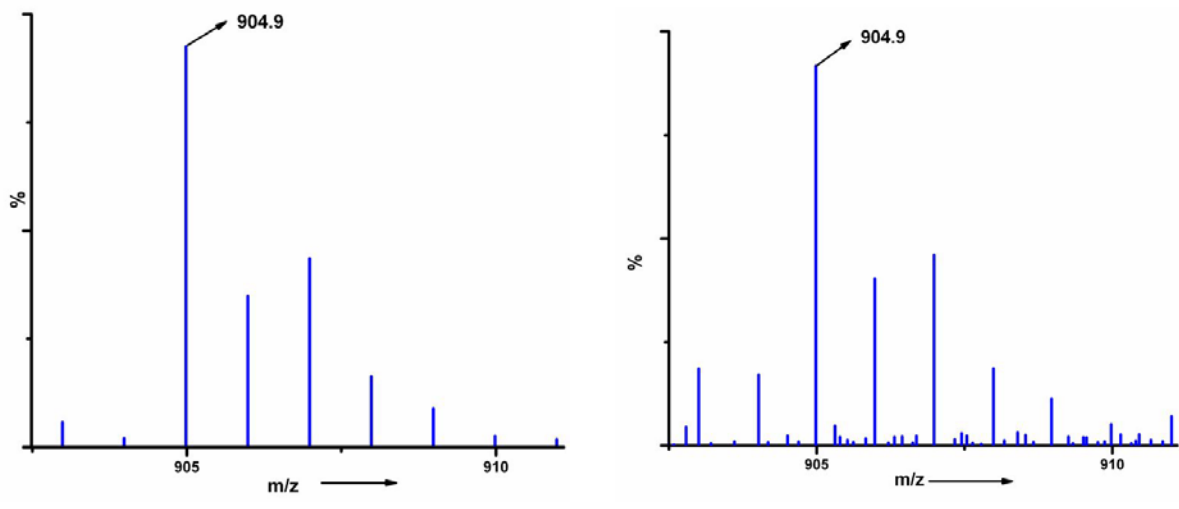


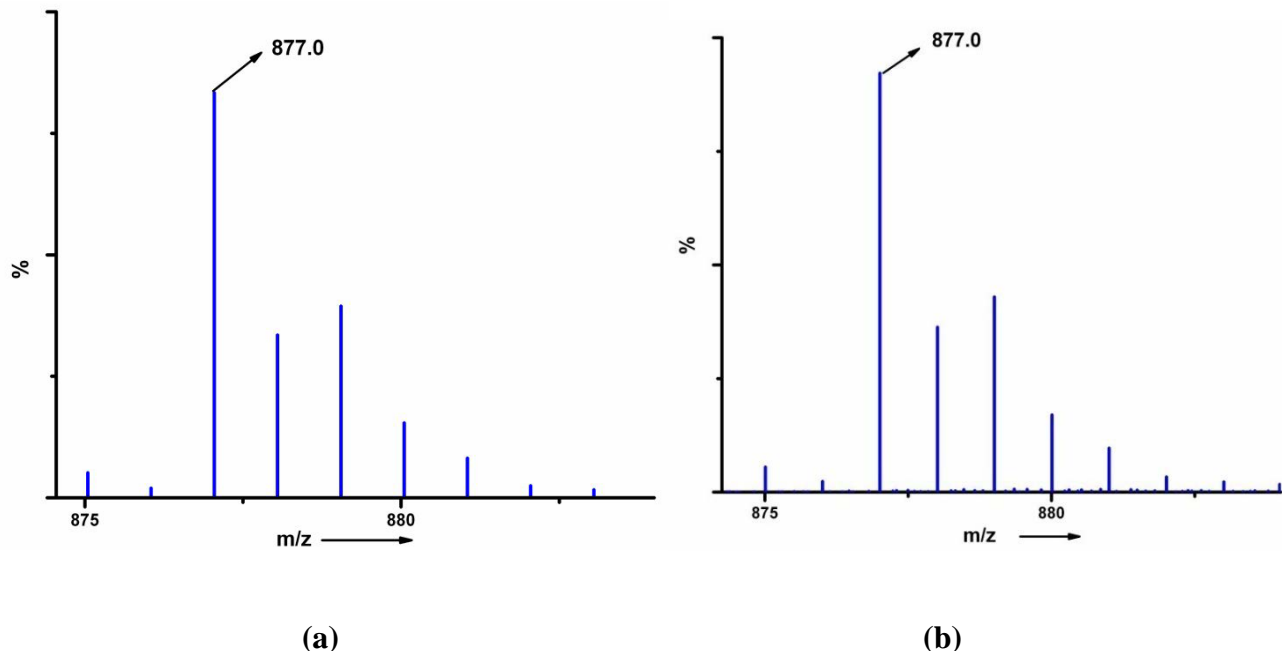
Figure S5. Molecular structure of **6**. Hydrogen atoms and solvent molecules are omitted for clarity.



(a)

(b)

Figure S6. ESI-MS of **2**. (a) Theoretical simulation (b) Experimental spectrum.



(a)

(b)

Figure S7. ESI-MS of **3**. (a) Theoretical simulation (b) Experimental spectrum.

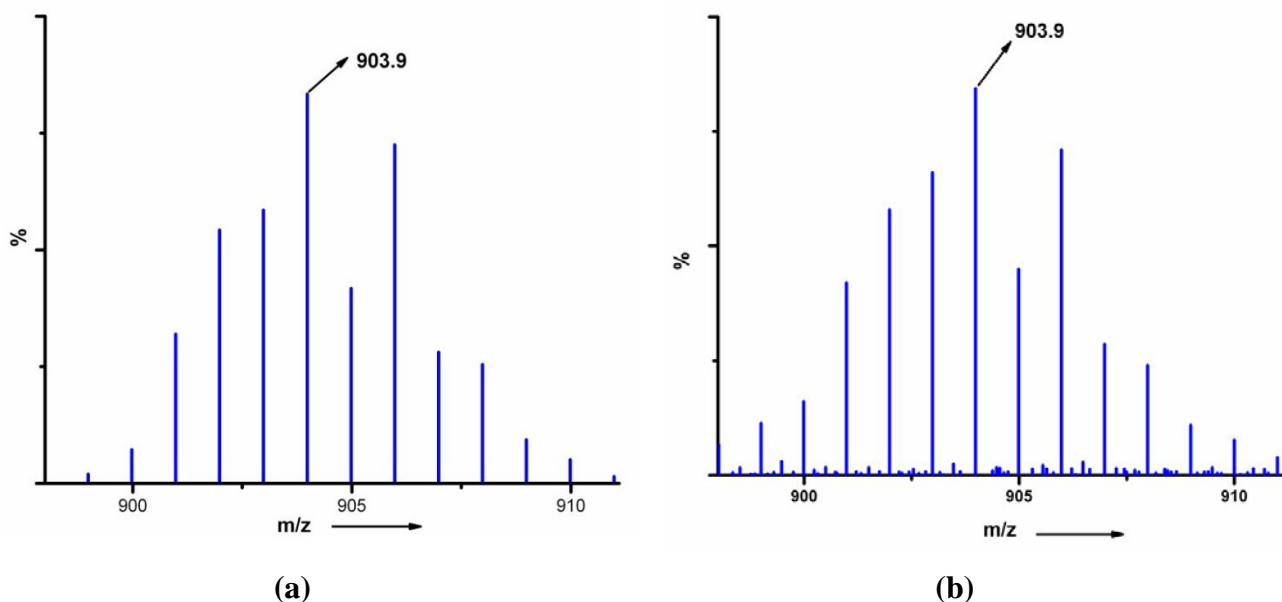


Figure S8. ESI-MS of **4**. (a) Theoretical simulation (b) Experimental spectrum.

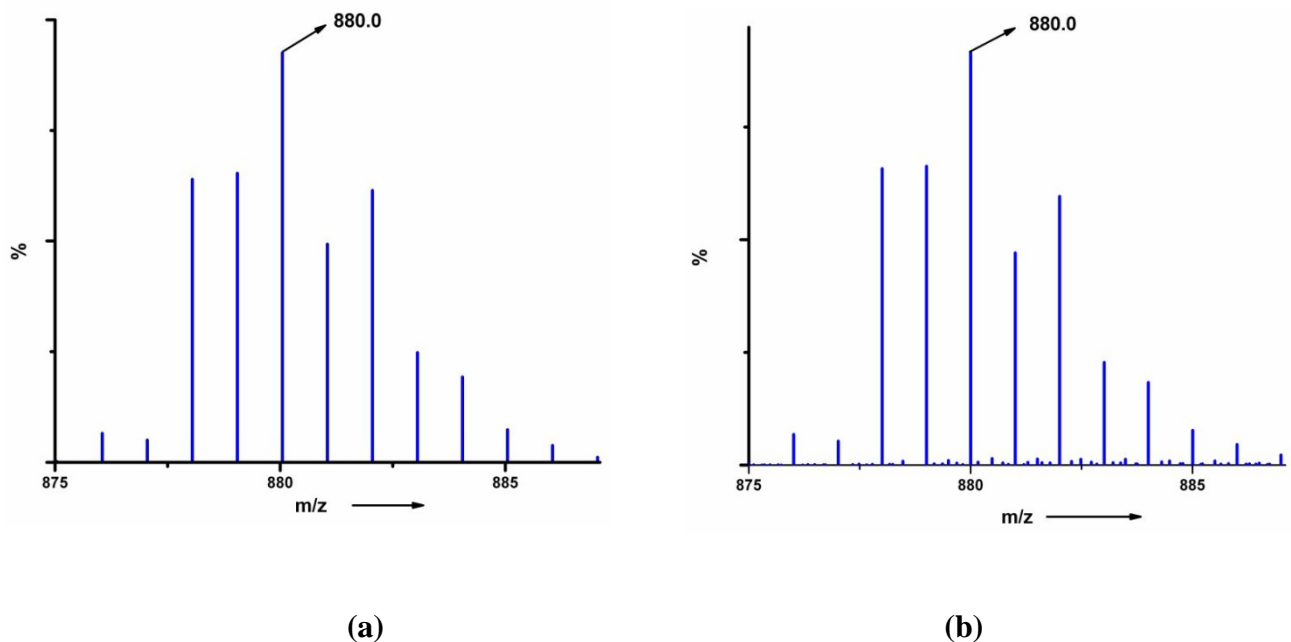


Figure S9. ESI-MS of **5**. (a) Theoretical simulation (b) Experimental spectrum.

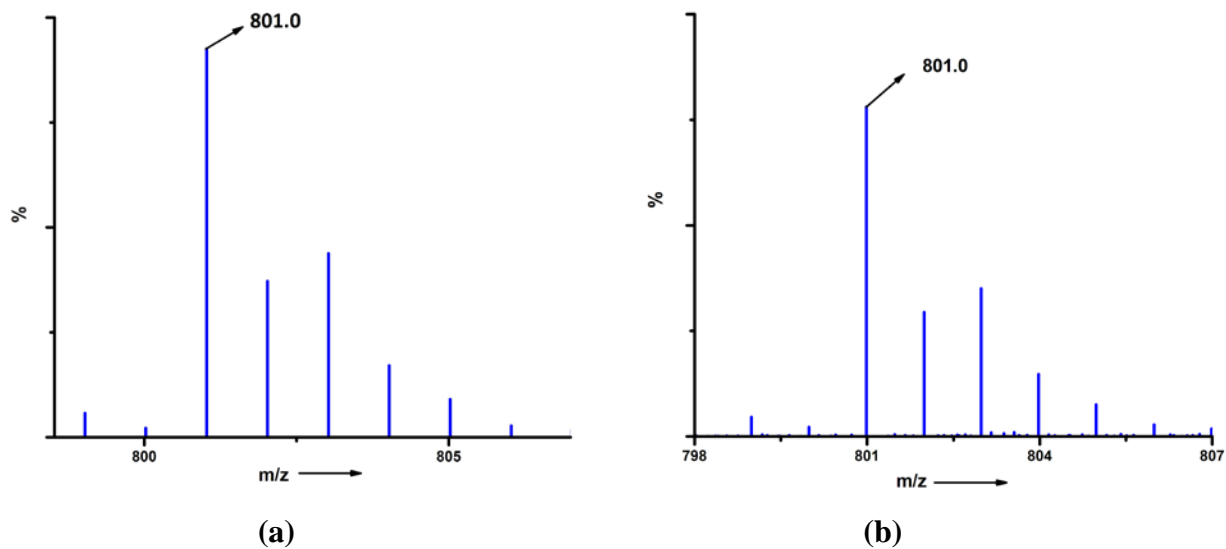


Figure S10. ESI-MS of **6**. (a) Theoretical simulation (b) Experimental spectrum.

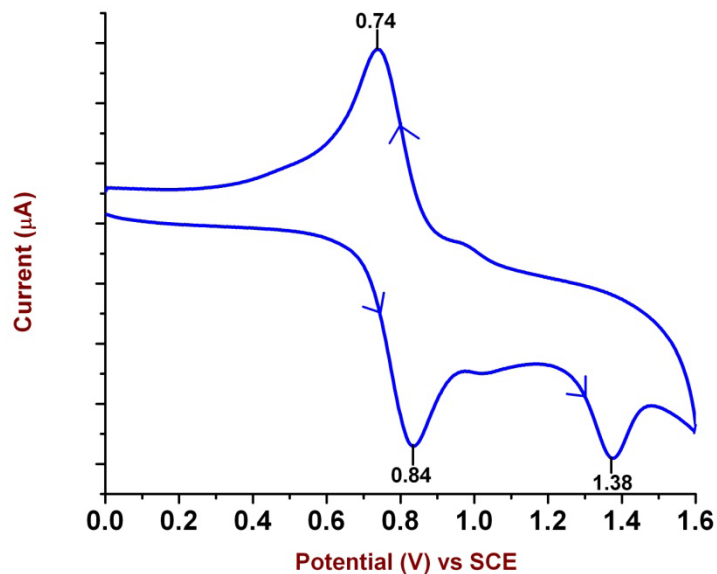


Figure S11. Cyclic voltammogram of **1** in CH_2Cl_2 using Glassy-Carbon working electrode and TBAP as supporting electrolyte (Scan rate 100mV/s).

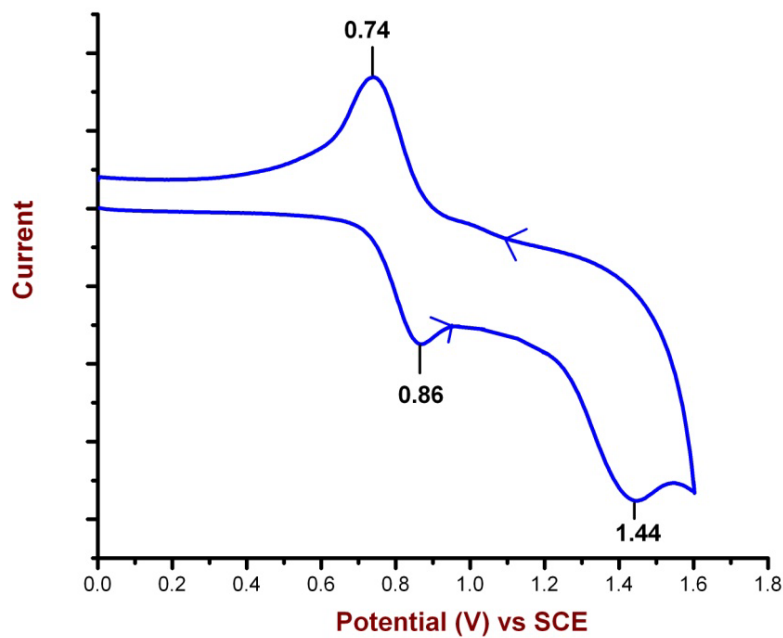


Figure S12. Cyclic voltammogram of **3** in CH_2Cl_2 using Glassy-Carbon working electrode and TBAP as supporting electrolyte (Scan rate 100mV/s).

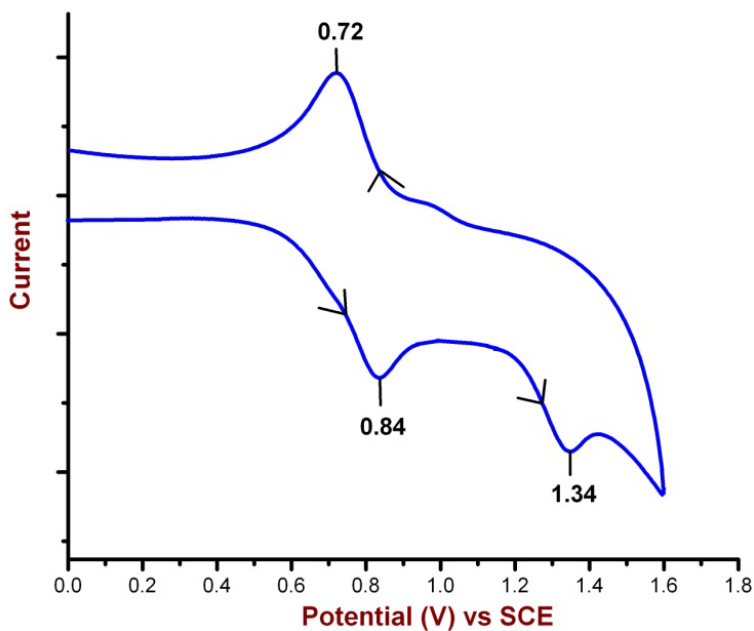


Figure S13. Cyclic voltammogram of **4** in CH_2Cl_2 using Glassy-Carbon working electrode and TBAP as supporting electrolyte (Scan rate 100mV/s).

Uv-vis Spectra:

The UV/Vis spectra of the ligand and the hetero metallic complexes were recorded at room temperature in CHCl_3 ($c \sim 4.1 \times 10^{-5}$). The observed λ_{\max} and corresponding ϵ_{\max} are summarized in Table S6. All the complexes shows similar type spectral features with a strong absorption around 284 nm along with two other transition around 354 nm and 444 nm, suggesting that these absorption bands arise due to spin allowed $\pi-\pi^*$ transitions in the ligand.

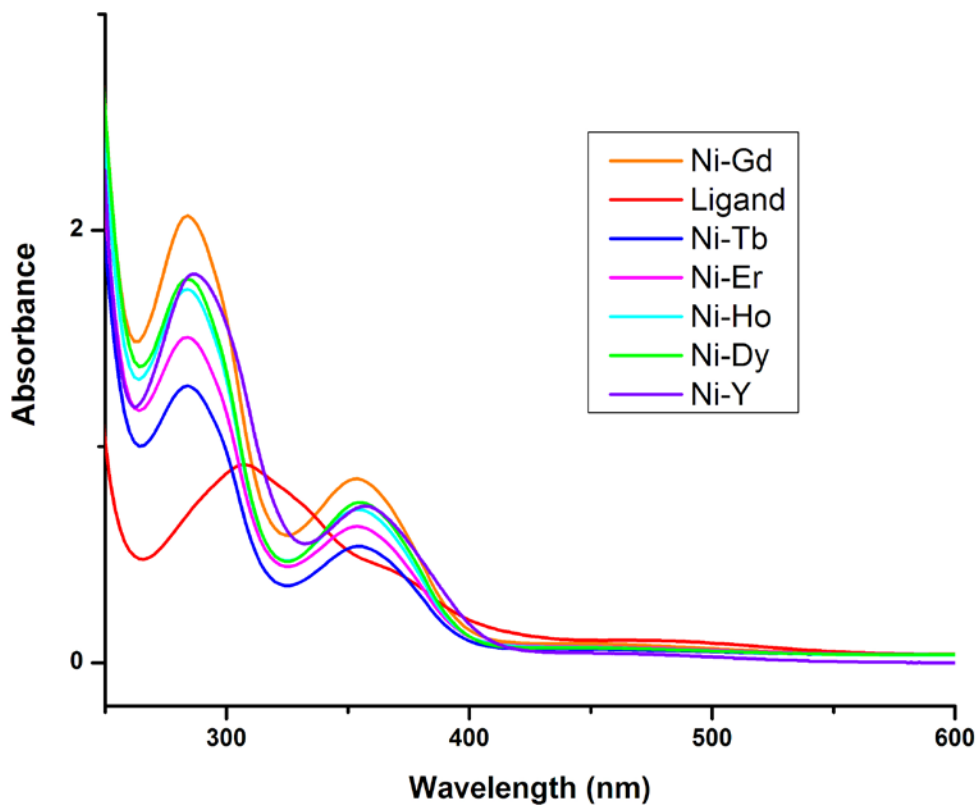


Figure S14. UV/Vis absorption spectra of ligand (H_2L) and complex (**1-6**).

Table S6. UV/Vis absorption data showing λ_{\max} value and corresponding ϵ_{\max} of ligand (H_2L) and complex (**1-6**).

Complex	ligand	Ni-Dy	Ni-Tb	Ni-Gd	Ni-Ho	Ni-Er	Ni-Y
$\lambda_{\max}(\text{nm})(10^{\text{-}})$ ${}^4\epsilon_{\max}$	306(2.23), 364(1.09), 469(0.25)	284(4.32), 354(1.80), 444(0.16)	284(3.12), 354(1.31), 443(0.15)	284(5.04), 355(2.07),449 (0.21)	284(4.21), 358(1.73), 451(0.17)	284(3.67), 354(1.5), 445(0.17)	286(4.38), 358(1.76), 450(0.11)

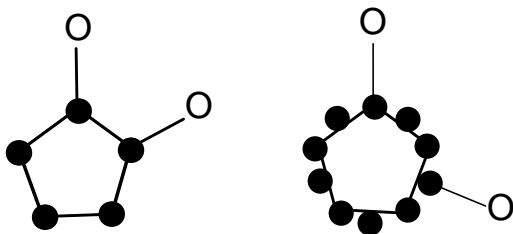


Figure S15. Conformations of the 1,1' disubstitutedferrocene.

^aSynclinal (eclipsed) conformation corresponds to the situation where the two cyclopentadienyl groups are perfectly eclipsed while the 1,1' substituents on these rings are not. In anticlinal (staggered) conformation the two cyclopentadienyl rings as well as two substituents on the 1,1' positions are staggered.

Table S7. Torsion angle data for H₂L and the complexes **1-6**.

Complex	ligand	Ni-Dy	Ni-Tb	Ni-Gd	Ni-Ho	Ni-Er	Ni-Y
θ°	2.16(5)	2.14(8)	3.25(5)	2.71(5)	2.60(3)	2.50(6)	3.169

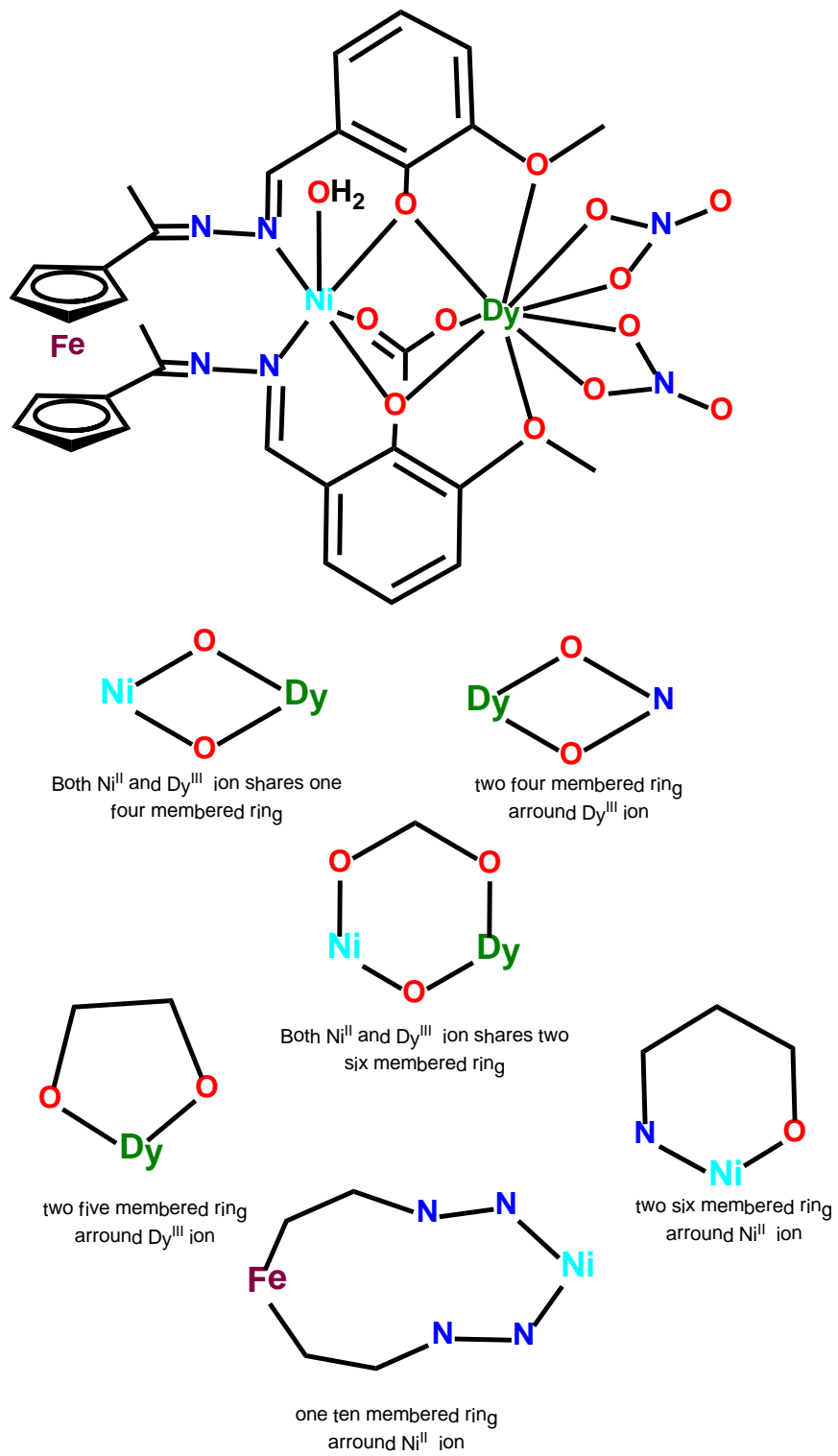


Figure S16. Varying sizes of rings found in complex 1.

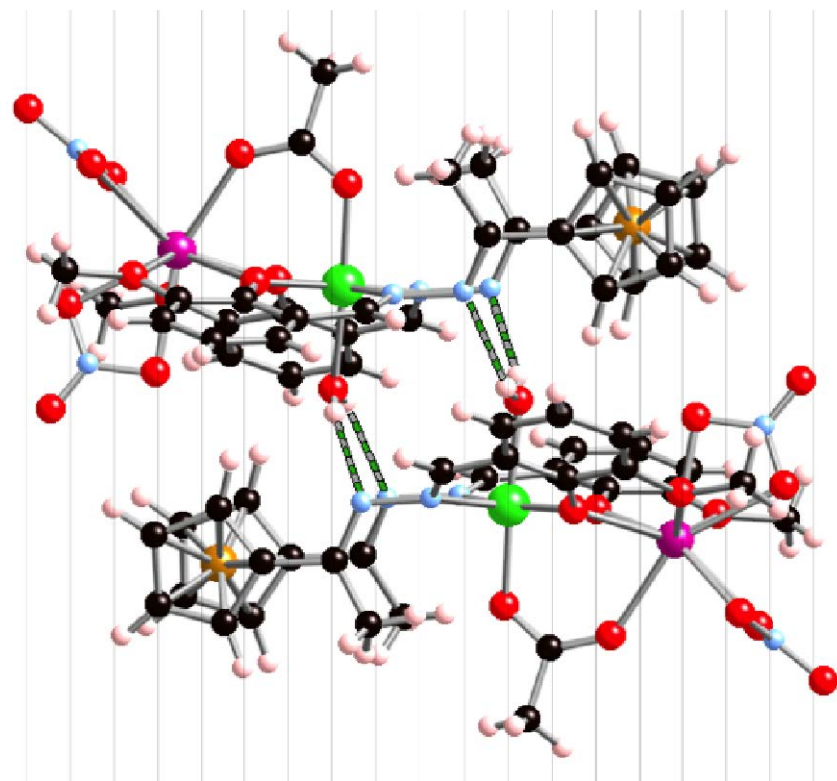
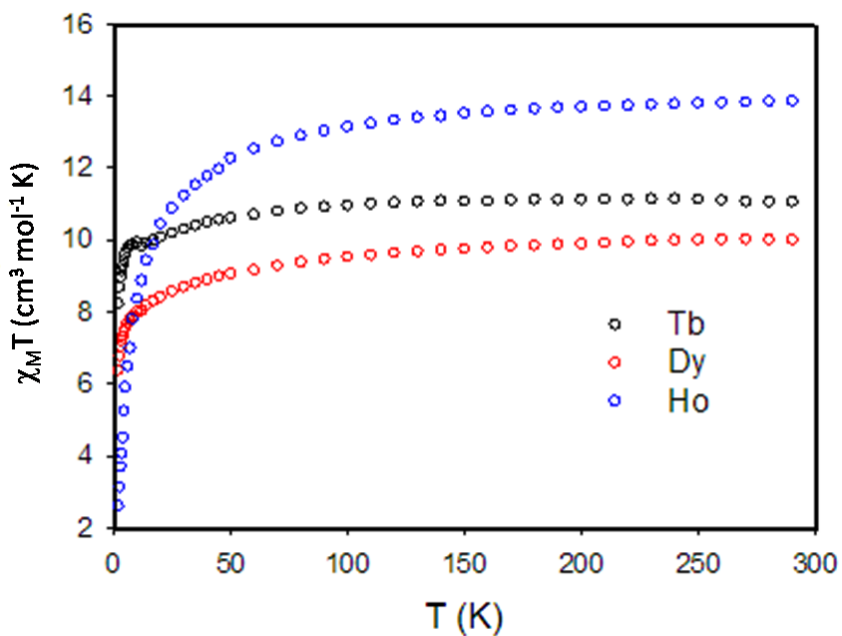
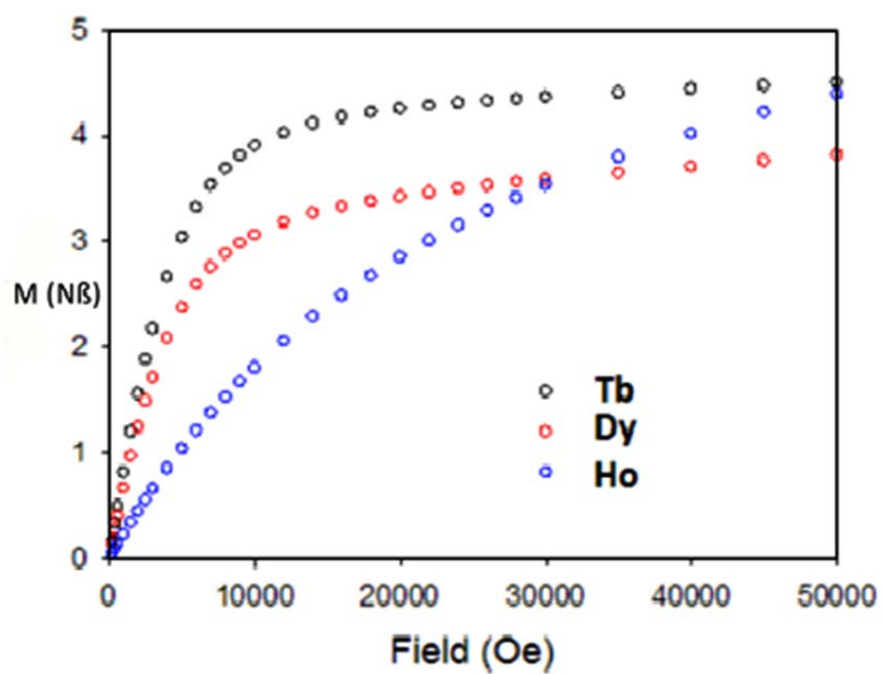


Figure S17. View of the H-bonds between two neighboring molecules of **4**.

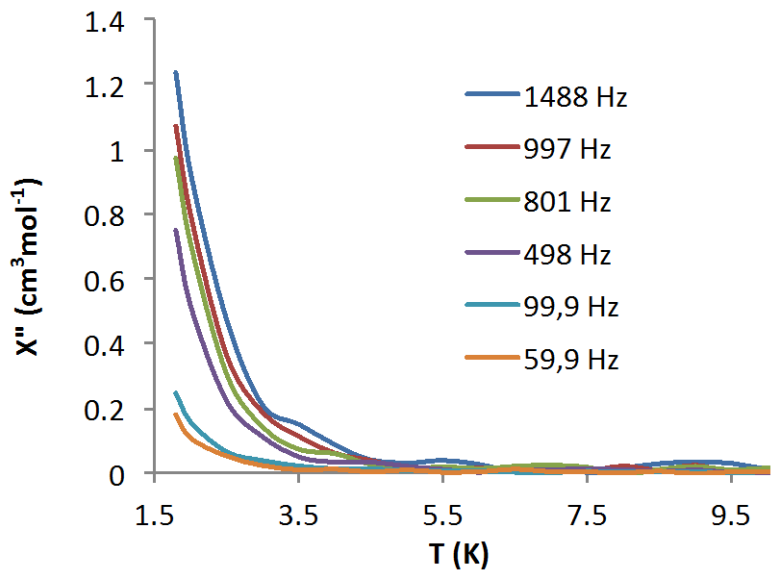


(a)

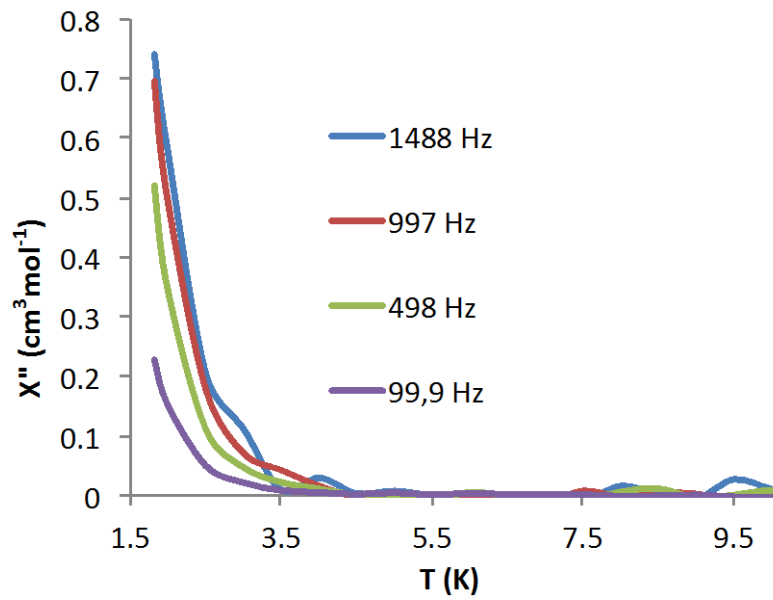


(b)

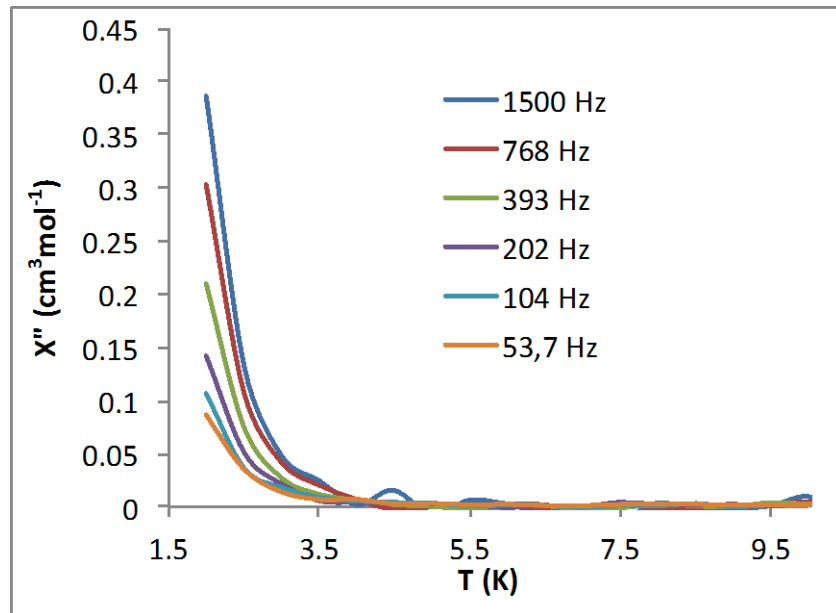
Figure S18. (a) χ_T vs. T plots for Zn-Ln complexes ($\text{Ln} = \text{Tb}, \text{Dy}$ and Ho); (b) $M=f(H)$ plots at 2 K for the ferrocene based Zn-Ln complexes ($\text{Ln} = \text{Tb}, \text{Dy}$ and Ho).¹⁴



(a)



(b)



(c)

Figure S19. $\chi'' = f(T)$ at dc field of 1000 Oe and ac field of 3 Oe at different frequencies for 1(a), 2(b) and 3(c) from top to down.